
Proceedings Paper:
Koshuriyan, Mohammad, Sescu, Adrian, Sassanis, Vasilis et al. (2016) Prediction of supersonic jet noise using non-parallel flow asymptotics and LES data within Goldstein's acoustic analogy. In: Studying Turbulence using Numerical Simulation Databases - XVI. Stanford University, Center for Turbulence Research, Stanford, California.

Prediction of supersonic jet noise using non-parallel flow asymptotics and LES data within Goldstein's acoustic analogy

By M. Z. Afsar†, A. Sescu‡, V. Sassanis‡, A. Towne, G. A. Brès‖ AND S. K. Lele

In this study we show how accurate jet noise predictions can be achieved within Goldstein's generalized acoustic analogy formulation for heated and un-heated supersonic jets using a previously developed asymptotic theory for the adjoint vector Green's function. In this approach, mean flow non-parallelism enters the leading order dominant balance producing enhanced amplification at low frequencies, which we believe corresponds to the peak sound at small polar observation angles. We determine all relevant mean flow and turbulence quantities using Large Eddy Simulations of two axi-symmetric round jets at fixed jet Mach number and different nozzle temperature ratios. Certain empirical coefficients that enter the turbulence length scales formula are tuned for good agreement with the far-field noise data. Our results indicate that excellent jet noise predictions are obtained using the asymptotic approach, remarkably, up to a Strouhal number of 0.5.

1. Motivation and objectives

Aeroacoustic modeling of jet noise within Goldstein's generalized acoustic analogy (GAA) formulation involves (a) solving the adjoint linearized Euler equations to determine the Green's function that defines the so-called propagator tensor and (b) appropriately modeling the Reynolds stress auto-covariance using experimental data and/or numerical simulations (Goldstein 2003). The far-field sound is then determined by the volume integral of an inner product of the propagator and the Reynolds stress auto-covariance tensors. This approach has proven to be successful for a number of test cases involving axi-symmetric round jets at a variety of acoustic Mach numbers and observation angles (Goldstein & Leib (2008) (hereafter referred to as G&L) and (Afsar 2010)). It has also shed light on what impact the mean flow field has on the far-field radiated sound for both heated and unheated flows (Afsar *et al.* 2011).

G&L's predictions were computed at $O(1)$ (i.e., arbitrary) frequencies for a propagator tensor based on a weakly non-parallel mean flow. Non-parallelism appeared in the analysis at supersonic speeds and only affected the solution within a thin critical layer where the adjoint vector Green's function is singular for the locally parallel mean flow. G&L constructed a uniformly valid composite solution for the adjoint Green's function, thus eliminating the critical-layer singularity that occurs when the observation angle, θ, is close to the downstream jet axis. They show that, as $\theta \to 0$, the dominant contribution to the propagator comes from the radial derivative of the Fourier transformed adjoint Green's function for the streamwise momentum perturbation. This was also confirmed by Karabasov *et al.* (2010)'s numerical calculations and by Afsar (2010) who, together

† Strathclyde University, UK
‡ Department of Aerospace Engineering, Mississippi State University
‖ Cascade Technologies Inc.

with G&L, showed that the acoustic efficiently of this term is raised to a dipole at low frequencies even though it appears as a quadrupole when multiplied by the appropriate Reynolds stress auto-covariance component in the acoustic spectrum formula (Goldstein 1975).

Physically, this behavior is due to the streamwise-radial, or '1-2', component of the fluctuating Reynolds stress multiplying the commensurate propagator component in such a manner that the latter possesses a pre-factor with directionality that scales as $\cos^4\theta/(1-\mathrm{M}(r)\cos\theta)^6$ (where $\mathrm{M}(r)$ is the local Mach number profile), which, obviously, peaks as $\theta \to 0$ (where θ is the polar observation angle), thus allowing an accurate prediction to be made of the peak jet noise that experiments show usually occurs at $\theta = 30^o$ in the forward arc. This result was derived in the matched-asymptotic-expansion sense, in which the solution for the pressure-like Green's function is divided into an inner region where the scaled radial coordinate $r/\sigma = O(1)$ and an $r = O(1)$ outer region with the scaled frequency, $\sigma = k^*_\infty \delta^* \ll O(1)$, being an asymptotically small parameter everywhere in the flow (δ^* is an appropriate dimensional length scale such as the nozzle radius and k_∞ is far-field wavenumber). Parallel flow asymptotics also showed that the components of the fluctuating Reynolds stress (other than '1-2') make a more dominant contribution to the large-angle-radiated sound at $O(1)$ frequencies under a general axisymmetric representation of the Reynolds stress auto-covariance tensor (such as that in (Afsar 2012)). This picture of jet noise is, however, oversimplified because it does not take into account mean flow spreading, which Karabasov *et al.* (2011) showed can be important at $O(1)$ Mach numbers and can increase the low-frequency radiation by as much as eight Decibels (dB) for $\theta = 30^o$ on a subsonic jet compared to the equivalent parallel flow solution of the GAA (adjoint linearized Euler) equations.

Goldstein, Sescu & Afsar (2012) (referred to herein as GSA) constructed an asymptotic solution to the adjoint vector Green's function problem in the GAA equations. As opposed to low-frequency asymptotics in a parallel flow discussed above, they considered a slowly diverging jet flow in which the spread rate, ϵ, is an asymptotically small parameter, $\epsilon \ll O(1)$. GSA determined that the only distinguished limit that could produce leading order changes to the acoustic spectrum is when the Strouhal number is of the same order as the jet spread rate. The resulting adjoint vector Green's function (and therefore the dominant '1-2' propagator component mentioned above) was different from the parallel flow result everywhere in the jet (not just in the critical layer as in G&L). Following on from GSA, Afsar *et al.* (2016) assessed the predictive capability of the asymptotics by using Reynolds-averaged Navier-Stokes (RANS) mean flow solutions to calculate the adjoint Green's function and the low-frequency asymptotically dominant propagator term in the GAA equations. Their main numerical result (figure 5.3a) confirms that an accurate prediction of the far-field sound can be made using this asymptotic approach. The predictions generally break down (i.e., rapidly decrease), however, above the peak Strouhal number (at $\mathrm{St} = 0.2$), but that is not altogether unexpected owing to low-frequency applicability of the theory.

In this paper our aim is to further investigate the applicability of the GSA asymptotics by considering the effect of heating and supersonic flow using large-eddy simulations (LES) of two axisymmetric round jets at a fixed jet Mach number of $\mathrm{M}_j = 1.5$. These solutions were reported in (Brès *et al.*, 2012; Brès *et al.*, 2016) and identified by the designations B118 and B122 for the unheated and heated configurations, respectively. The operating conditions are summarized in Table 1. In Section 2 we summarize the basic theory used in this work. In Section 3 we show the mean flow and turbulence

Experimental (Schlinker *et al.* 2012)	LES case	Description	M_j	TR	M_a
B118	A1	isothermal ideally-expanded	1.5	1.0	1.5
B122	A2	heated ideally-expanded	1.5	1.74	1.98

TABLE 1. Brès et al (2012) test cases.

properties for the 1212 component of the Reynolds stress auto-covariance tensor, and in section 4 we show how excellent jet noise predictions can be made using the asymptotic model up to a maximum Strouhal number of about 0.6.

2. Application of Goldstein-Sescu-Afsar asymptotic theory to heated jets

Suppose that all lengths have been normalized by the nozzle radius, r_j, and all velocities by the mean jet exit velocity, U_j. Let the pressure p, density ρ, enthalpy h, and speed of sound c satisfy the ideal gas law equation of state $p = \rho c^2/\gamma$ and $h = c^2/(\gamma - 1)$, where γ denotes the ratio of specific heats. Afsar *et al.* (2016) applied the GSA asymptotic theory within the GAA formalism to show that the low-frequency acoustic spectrum at the observation point $\boldsymbol{x}$ due to momentum transfer by the fluctuating Reynolds stress in an axi-symmetric round turbulent jet flow of volume $V(\boldsymbol{y})$ is given by the algebraic result

$$I_{\omega}^{\mathrm{LOW}}(\boldsymbol{x}) \to \left(\frac{\epsilon}{2c_{\infty}|\boldsymbol{x}|}\right)^2 |\tilde{G}_{12}(\boldsymbol{y}|\boldsymbol{x};\omega)|^2 \Phi_{1212}(\boldsymbol{y};\omega) \tag{2.1}$$

as $|\boldsymbol{x}| \to \infty$. In this formula, the cylindrical polar coordinates $\boldsymbol{y} = (y_1, r, \psi)$ are defined with respect to an origin at the nozzle exit plane. Equation (2.1) will continue to hold in heated jets when mean flow quantities and turbulence parameters are appropriately defined.

2.1. *The propagator solution*

The adjoint Green's function enters through the propagator component, $\tilde{G}_{12}(\boldsymbol{y}|\boldsymbol{x};\omega)$, defined as

$$\tilde{G}_{12}(\boldsymbol{y}|\boldsymbol{x};\Omega) = \frac{\partial \tilde{G}_1}{\partial r} - \tilde{G}_4 \frac{\partial U}{\partial r} \tag{2.2}$$

for the Favre-averaged mean flow $\tilde{v} = \overline{\rho \boldsymbol{v}}/\bar{\rho} = (U, V_r)(\boldsymbol{y})$ that depends on y_1 through the slow streamwise coordinate $Y = \epsilon y_1 = O(1)$ for a jet of an asymptotically small spread rate, $\epsilon \ll O(1)$. The mean flow then divides into an inner region given by slowly varying mean flow expansion formulae, Eqs. (13)-(17) in (Afsar *et al.* 2016) (or, Eqs. (3.1)-(3.4) in GSA), where $r = |y_T| = \sqrt{y_2^2 + y_3^2} = O(1)$, and an outer region at radial distances, $R = \epsilon r = O(1)$. The propagator component $\tilde{G}_{12}(\boldsymbol{y};\Omega)$ is then defined at the particular scaled temporal frequency, $\Omega = \omega/\epsilon = O(1)$, shown by GSA to be where mean flow non-parallelism changes the leading-order structure of the adjoint Green's function solution everywhere in the flow (and not just in the critical layer at supersonic speeds as in G&L's solution) and at $O(1)$ Mach numbers. This distinguished limit follows supposing that the space-time adjoint vector Green's function variable, $g^a_{\nu 4}(\boldsymbol{y}, \tau|\boldsymbol{x}, t)$, depends on time, τ, through the $O(1)$ slowly breathing time $T = \epsilon\tau$ (cf. Wu & Huerre 2009). Therefore, the Strouhal number, St, is of the order of the jet spread rate, ϵ, in the solution of Fourier transform of $g^a_{\nu 4}(\boldsymbol{y}, \tau|\boldsymbol{x}, t)$ (Eqs. (7)-(9) in (Afsar *et al.* 2016)).

The asymptotic structure of the adjoint Green's function is then identical to the mean

flow in that it also divides into an inner solution in the region where the radial distance $r = O(1)$ and into an outer solution in the region where $R = \epsilon r = O(1)$. The richest inner equations are found by the non-trivial dominant balance of $g^a_{\nu 4}(\boldsymbol{y}, \tau|\boldsymbol{x}, t)$ given by Eqs. (5.5)-(5.6) in GSA. The scaled Fourier transform of $g^a_{\nu 4}(\boldsymbol{y}, \tau|\boldsymbol{x}, t)$ for $\nu = (1, 4, 5)$ then satisfies Eqs. (18)-(21) for the leading-order azimuthal mode expansion since higher-order azimuthal modes produce an asymptotically small (i.e., $o(\epsilon)$) correction to these inner equations. However, tremendous simplification can be achieved by taking (Y, U) rather than (Y, r) as the independent variables of choice. The implicit function theorem shows that $\boldsymbol{y} = (Y, r)$ can be implicitly related to the field space $\boldsymbol{y} = (Y, U(Y, r))$ and that the Green's function variable $\tilde{G}_i(\boldsymbol{y}|\boldsymbol{x}; \Omega) = (\tilde{G}_1, \tilde{G}_4)(\boldsymbol{y}|\boldsymbol{x}; \Omega)$ then depends on $(\boldsymbol{y}; \Omega)$ through field space $(Y, U(Y, r); \Omega) \equiv (Y, r; \Omega)$. GSA showed that the one-to-one transformation of independent variables, $(Y, r) \to (Y, U)$, can be used together with the chain rule to combine the inner equations to the second-order hyperbolic partial differential equation

$$\widetilde{c^2} \frac{\partial}{\partial U} \left(\frac{1}{\widetilde{c^2}} \bar{D}_0 \bar{\nu} \right) + \tilde{X}_1 \frac{\partial^2 \bar{\nu}}{\partial U^2} = 0, \tag{2.3}$$

in which $Y = \text{const.}$, $dU/dY = \tilde{X}_1/U$ are characteristic curves (Garabedian (1998), pp. 121-122). This equation requires that $\widetilde{c^2}(Y, r) = f(U)$ and satisfies Crocco's relation, and for a composite Green's function variable $\nu = \widetilde{c^2}\tilde{G}_4 + \tilde{G}_5$. But the Crocco-Busemann relation (see equation 2.4c in (Leeshafft, Huerre, Sagaut & Rerracol 2006)), which applies when the jet flow is heated, shows that the mean speed of sound is still a function of $U(Y, r)$. Therefore, Eq. (2.3) will continue to hold in such a case. The advantage of solving this equation to determine the low-frequency structure of the adjoint linearized Euler equations (Eqs. (4.8)-(4.10) of G&L) is clear. The hyperbolic structure of equation (2.3) shows that it is unnecessary to impose a downstream boundary condition. Figure 1 in GSA indicates how information propagates to both the left and the right from the $U = 0$ boundary and that no boundary conditions are required on the $Y = 0$ and $Y \to \infty$ boundaries (i.e., no inflow boundary condition is required here). Hence the solution for the composite variable $\nu(Y, U)$ is now uniquely determined by the outer boundary conditions (i.e., by matching to the inner limit of the outer solution using the Van Dyke (1975) rule)

$$\nu(0, Y) \to -i\Omega c_\infty^2 e^{-i\Omega Y \cos\theta / c_\infty} \tag{2.4}$$

$$\frac{\partial \nu}{\partial U}(0, Y) \to -i\Omega c_\infty \cos\theta e^{-i\Omega Y \cos\theta / c_\infty} \tag{2.5}$$

on the non-characteristic curve $U = 0$, with $Y \geq 0$ (where, as indicated above, $U \to 0$ corresponds to outer limit, $r \to \infty$). The coefficient $\tilde{X}_1$ is the streamwise component of the mean flow advection vector (equation 5.15 in GSA) and $\bar{D}_0 = i\Omega + U\partial/\partial Y$.

The inner solution $\nu(U, Y)$ is then induced by incoming waves by the outer wave equation. For the $O(\Omega^0)$ solution, any influence of the nozzle (i.e., via the scattered wave contribution to the outer solution) can be neglected because the inner solution, which generates the scattered waves, will not behave logarithmically as $r \to \infty$ when matched to the outer solution. The logarithmic behavior of the axi-symmetric mode of the scattered solution (Eq. (5.2) in GSA) follows from the small argument expansion for the solution to the two-dimensional Helmholtz equation (Morse & Feshbach (1953), p. 891) in the outer region. Using Van Dyke's rule, this expansion shows that $\nu(0, Y)$ will not match onto the transcendental lnR behavior as $R \to 0$ at $O(\Omega^0)$.

2.2. *Turbulence modeling*

The turbulence enters the acoustic spectrum formula, Eq. (2.1), through the spectral tensor component $\Phi_{1212}(\boldsymbol{y};\omega)$ defined by the space-time Fourier transform

$$\Phi_{1212}(\boldsymbol{y};\omega) = \frac{1}{2\pi}\int_{V(\boldsymbol{\eta})}\int_{-\infty}^{\infty} R_{1212}(\boldsymbol{y},\boldsymbol{\eta};\tau)e^{i(\boldsymbol{k}.\boldsymbol{\eta}-\omega\tau)}\,d\boldsymbol{\eta}\,d\tau, \tag{2.6}$$

where the $R_{1212}(\boldsymbol{y},\boldsymbol{\eta};\tau)$ component of the Reynolds stress auto-covariance tensor is given by the time-average

$$R_{1212}(\boldsymbol{y},\boldsymbol{\eta};\tau) = \lim_{T\to\infty}\frac{1}{2T}\int_{-T}^{T}\left[\rho v_1' v_2' - \overline{\rho v_1' v_2'}\right](\boldsymbol{y},\tau)\left[\rho v_1' v_2' - \overline{\rho v_1' v_2'}\right](\boldsymbol{y}+\boldsymbol{\eta},\tau+\tau_0)\,d\tau_0. \tag{2.7}$$

In Section 3 we show the streamwise development of $R_{1212}(\boldsymbol{y},\boldsymbol{\eta};\tau)$ at various radial locations in the jet using the Brès et al. data. Construction of $R_{1212}(\boldsymbol{y},\boldsymbol{\eta};\tau)$ using an exponential model with algebraic tails and the subsequent calculation of $\Phi_{1212}(\boldsymbol{y};\omega)$ is worked out in Afsar *et al.* (2016), and we use their final result

$$\Phi_{1212}(\boldsymbol{y};\omega) = 2\pi A_{1212}(\boldsymbol{y})\left(\frac{l_0 l_1 l_2 l_3}{\chi^2 U_c}\right)\times \tag{2.8}$$

$$\left[(a_0-a_1-a_2)+(a_1\tilde{\omega}^2-\bar{k}_1(\tilde{\omega}(a_1-a_2)(l_1/l_0)-a_1\bar{k}_1))(4/\chi)\right] \tag{2.9}$$

where $\chi(\tilde{\omega},\bar{k}_1)=\bar{k}_1^2+\tilde{\omega}^2+1=(k_1-\tilde{\omega}(l_1/l_0))^2+\tilde{\omega}^2+1$ and $\tilde{\omega}=(\omega l_0/U_c)$ is the normalized temporal frequency where U_c is the convection velocity of the turbulence. The length scales in Eq. (2.9) are taken to be proportional to the local turbulent kinetic energy $k(\boldsymbol{y})$ and the rate of energy dissipation $\tilde{\epsilon}(\boldsymbol{y})$ as $l_i(\boldsymbol{y}) = c_i(k^{3/2}/\tilde{\epsilon})(\boldsymbol{y})$ for $i=0,1,2,3$. We obtain all the mean flow from the LES calculation rather than scaling a RANS mean flow as done by Karabasov *et al.* (2010).

3. Streamwise development of mean flow and Reynolds stress auto-covariance

In Figure 1, we show the Favre-averaged mean flow fields, $(U,V_r,\tilde{X}_1)(\boldsymbol{y})$, as a two-dimensional field for both B118 (cold) and B122 (hot) jets. The LES data was averaged over a time span of 0.032 s for the B118 case and 0.0176 s for the B122 case (corresponding to 321 and 168 time units D/U_j, respectively) to obtain a converged mean flow, which was then averaged over each 24-azimuthal plane to obtain an azimuthally averaged mean flow. Comparison of Figure 1a and Figure 1b shows that heating slightly reduces the potential core length while increasing the magnitude of the radial velocity V_r (Figures 1(c,d)) and localizing it closer to the nozzle lip line. However, given these differences, the distribution of the mean flow advection operator $\tilde{X}_1$ in Figure 2 appears to be relatively unchanged in shape; its magnitude associated with the heated jet (Figure 2b) is slightly higher in the vicinity of the nozzle lip.

Figure 3 shows the Reynolds stress auto-covariance tensor component R_{1212} as a function of the time delay τ for different streamwise shifts η_1, where the radial shift η_2 is set to zero. The plots are taken at a fixed streamwise location ($y_1=8$) and four different radial locations ($r=0.25,0.5,0.75,1.0$). Figure 3 indicates that the negative dip (sometimes referred to as the de-correlation) in R_{1212} is largely negligible and (a_1,a_2) can be set to zero in Eq.(2.9). A comparison of the different plots in Figure 3 suggests that the correlation increases in strength as r increases, which may also indicate an increase in the length scales (which can be calculated by taking the integral of correlations). There

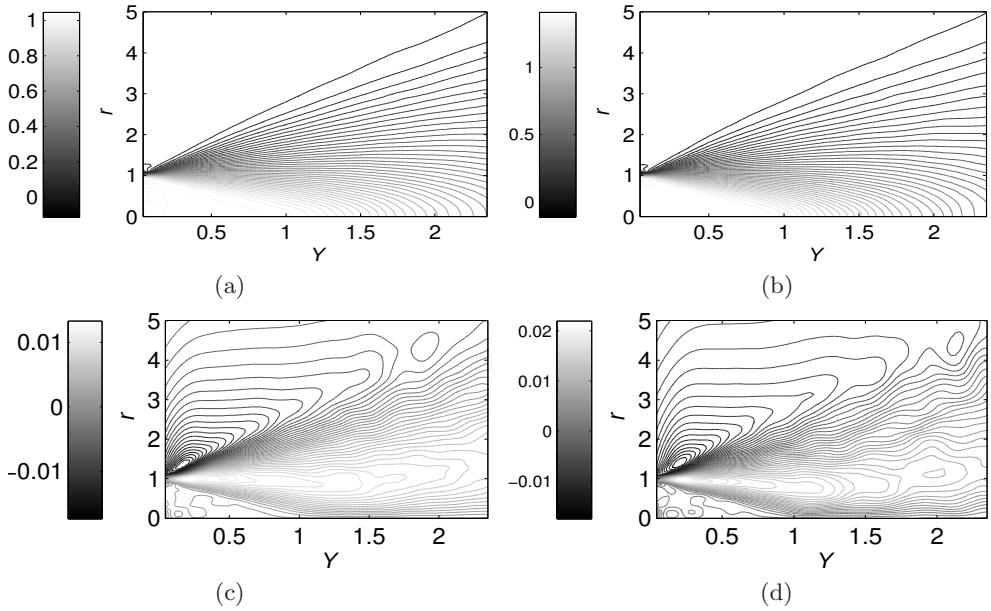

FIGURE 1. Mean flow: (a) B118, $U(Y,r)$, (b) B122, $U(Y,r)$, (c) B118, $V_r(Y,r)$ (d) B122, $V_r(Y,r)$.

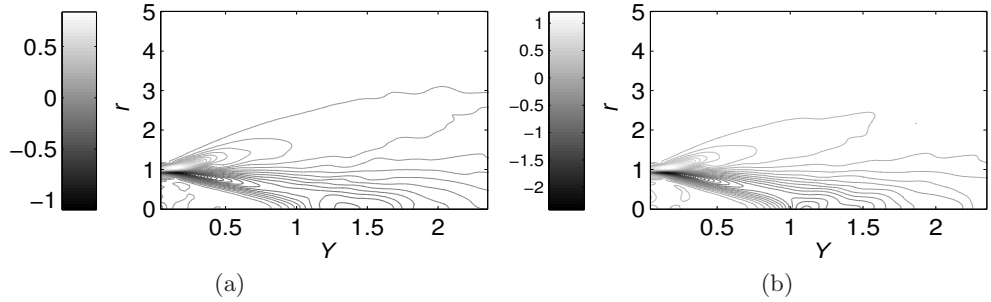

FIGURE 2. Spatial distribution of $\tilde{X}_1$ (a) B118; (b) B122.

is no appreciable difference in the rate of decay of the correlations with heating; in other words, the normalized shape of R_{1212} curves is similar. The absolute magnitude of R_{1212} does, of course, change (it increases) as the jet is heated and this directly impacts the magnitude of the acoustic spectrum contours through the change in $k(\boldsymbol{y})$.

Figure 4 shows the contours of $\tilde{G}_{12}$ at the peak frequency of St = 0.2 for B118 and B122 jets. The convergence of the numerical algorithm applied to Eq. (2.3) was analyzed in GSA and Afsar *et al.* (2016), and it was found to be within 5% at almost all regions of the jet, with only slight differences in results coming near the inner boundary as $U \to 1$. In Figures 5(a,b) we show contour plots of the acoustic spectrum rI_{low}. The indication here is that the peak noise source lies near $y_1 \sim 6$ or $Y \sim 1$. The absolute magnitude of the acoustic spectrum is greater with heating (at fixed M_j), which is consistent with the noise measurements of a heated flow at constant jet Mach number that shows an increase in noise of almost 10dB with heating.

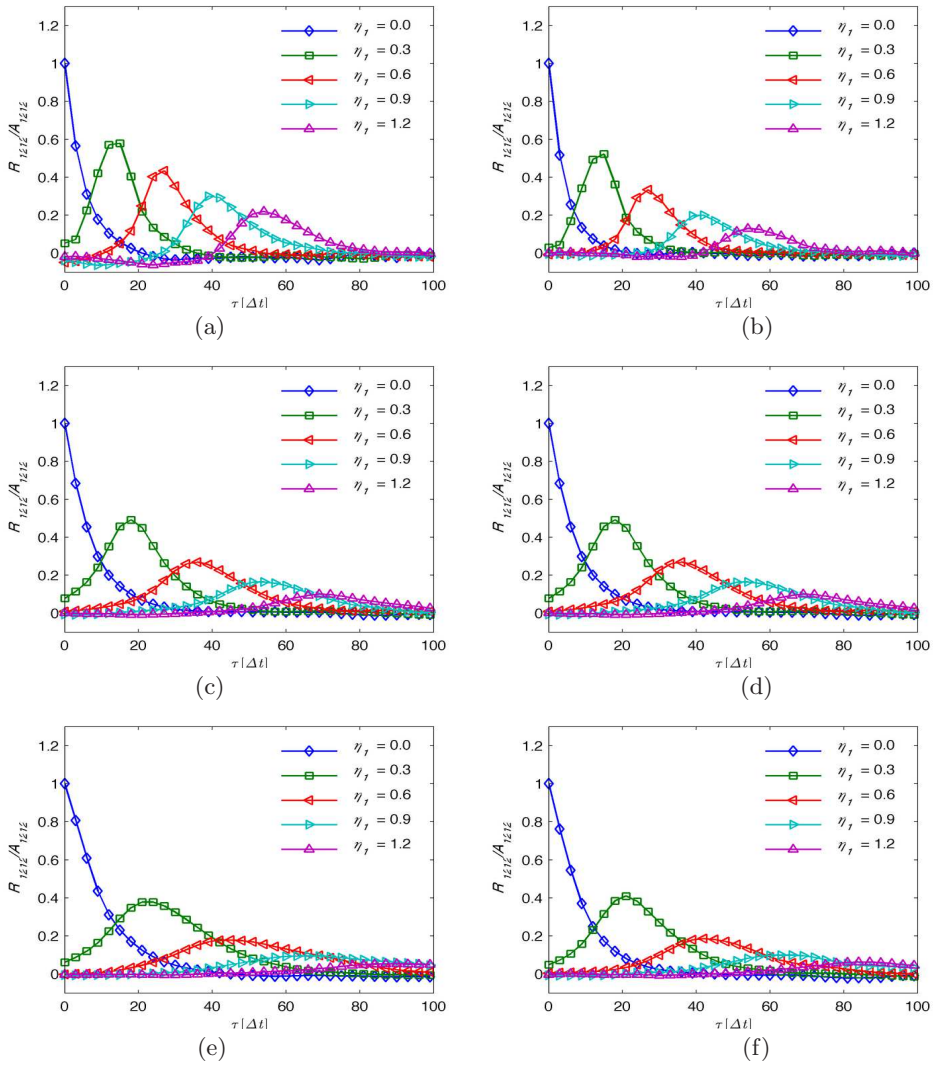

FIGURE 3. $R_{1212}(\boldsymbol{y}, \boldsymbol{\eta}; \tau)/R_{1212}(\boldsymbol{y}, \mathbf{0}; 0)$ at $y_1 = 8$ and four radial locations: (a) and (b) $r = 0.25$, (c) and (d) $r = 0.5$, (e) and (f) $r = 0.75$. Left column is B118 and right column is B122.

4. Jet noise predictions

Our experimentation with the parameters in the model showed that it is possible to achieve remarkably accurate noise predictions of both unheated and heated jets, with $(a_0, a_1, a_2) = (1.0, 0, 0)$ in Eq (2.9); i.e., a purely positive correlation that is consistent with the very small (if not negligible) de-correlation in R_{1212} with time delay and spatial separation displayed in Figure 3. Hence, only three parameters are needed in the turbulence model, namely the length scale parameters in Eq (2.9). But given that Figure 3 also shows very little difference in the streamwise space-time structure of R_{1212}, we keep $(c_0, c_1) = (0.15, 1.0)$ the same in both cases and vary only c_2 (where $c_2 = c_3 = c_\perp$), which is related to the transverse length scales. Specifically, we set $c_2 = 0.17$ for B118

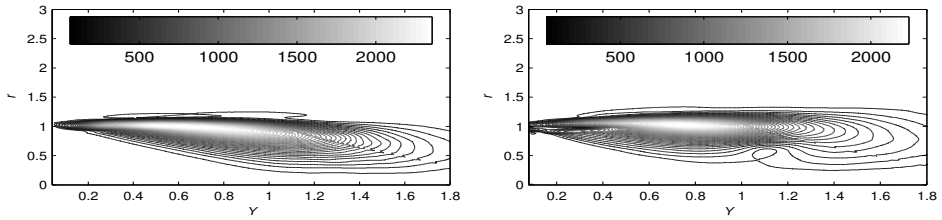

(a) (b)

FIGURE 4. Contours of $|\tilde{G}_{12}|$: (a) B118, (b) B122.

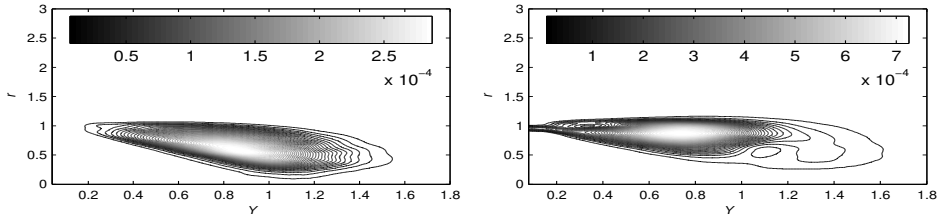

(a) (b)

FIGURE 5. Contours of $rI_{\omega}^{\mathrm{LOW}}$ at St = 0.2 and $\theta = 30$ deg: (a) B118, (b) B122.

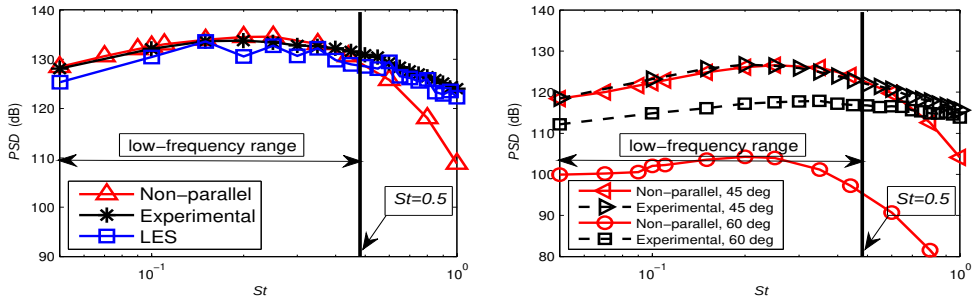

(a) (b)

FIGURE 6. Acoustic spectra for B118: (a) $\theta = 30$ (b) $\theta = 45$ and 60.

and $c_2 = 0.09$ for B122. Remarkably, these parameter values provide accurate predictions for the cold jet up to St ~ 0.5, which is beyond what was obtained by Afsar *et al.* (2016).

In Figures 6 and 7 we show the acoustic spectrum (dB) for B118 and B122, respectively, compared against experimental data (see Schlinker *et al.* (2012), Brès *et al.* (2012) and Brès *et al.* (2016)). As mentioned, the spectrum for the observation angle $\theta = 30$ deg shows very promising agreement with experimental and LES results at low frequencies (almost up to St $= 0.6$). When the same set of parameters are used for larger angles ($\theta = 45, 60$ deg), the acoustic spectrum predictions (shown in Figure 6) are no longer in agreement, but this is not surprising since the theory in its current form is supposed to provide accurate predictions at small observation angles. In Figure 7(b) we show the senstivity of the 30° prediction for B122 (heated) jet at various values of parameter c_2. Any predictions in the heated case must be interpreted as a first approximation since Eq. (2.1) does not include auto-variances and co-variances associated with enthalpy flux and momentum flux/enthalpy flux coupling, respectively (Afsar *et al.* 2011).

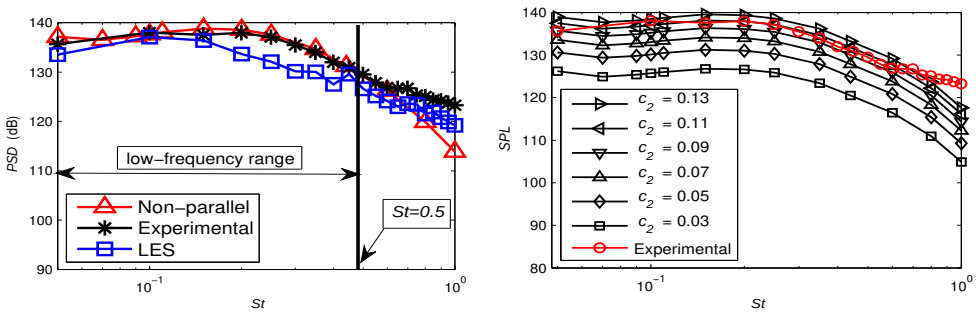

(a) (b)

FIGURE 7. Acoustic spectra for B122: (a) $\theta = 30^0$ and (b) sensitivity to c_2.

5. Conclusions

Goldstein-Sescu-Afsar postulated that the appropriate distinguished limit in which non-parallel mean flow effects introduce a leading-order change in the propagator tensor in the generalized acoustic analogy equations must be when the jet spread rate is of the same order as the Strouhal number. In this paper we have extended the Afsar *et al.* (2016) analysis to show that this approach, i.e., Eq. (2.1), remains valid in heated jets since the assumption that $\widetilde{c^2}(Y, r) = f(U)$ in which $\widetilde{c^2}$ is given by the Crocco-Busemann relation, continues to remain valid in heated jet flows. Our results have shown that the theory not only provides a means to understand, qualitatively, the effects of non-parallelism within the acoustic analogy but also provides excellent predictive capability of the jet noise. The reduced form of the acoustic spectrum formula (equation 19 in (Afsar *et al.* 2011)) used here is limited to low frequencies and shallow downstream observation angles from the jet axis. The results in this paper indicate that the 30° spectrum can be accurately predicted in both the unheated (B118) and heated (B122) cases, remarkably, up to a Strouhal number of almost 0.6. While the parameters in the turbulence model (Eq (2.9)) do require revisiting, particularly to obtain a precise estimation of the length scales, the approach does show the usefulness of the asymptotic theory as part of a realistic prediction code. Future work will address these issues, namely to reconstruct the spectrum of the Reynolds stress auto-covariance component R_{1212} directly from LES data without the need of any modeling whatsoever (i.e., by Fourier transforming the R_{1212} correlation function data as necessary using Eq (2.6)). In addition, the higher polar angle predictions can be improved by including the other components of the axi-symmetric representation of the generalized auto-covariance tensor, $R_{\mu j \nu l}$, which includes enthalpy fluctuations when Greek suffixes $(\mu, \nu) = 4$.

Acknowledgments

The authors would like to thank Prof. Parviz Moin for supporting this work. We warmly acknowledge the assistance provided by Prof. Joe Nichols (University of Minnesota) in the initial post-processing of the LES data. We would also like to thank Dr. S. J. Leib (Ohio Aerospace Institute) for providing us with the spectral tensor routines. The LES studies were supported by the NAVAIR STTR project under the supervision of Dr. John T. Spyropoulos. The main calculations were carried out at DoD HPCMP supercomputer facilities in ERDC DSRC.

REFERENCES

Afsar, M. Z., Goldstein, M. E. & Fagan, A. M. 2011 Enthalpy-flux/momentum-flux coupling in the acoustic spectrum of heated jets. *AIAA J.* **49**, 2252–2262.

Afsar, M. Z. 2010 Asymptotic properties of the overall sound pressure level of sub-sonic air jets using isotropy as a paradigm. *J. Fluid Mech.* **664**, 510–539.

Afsar, M. Z. 2012 Insight into the two-source structure of the jet noise spectrum using a generalized shell model of turbulence. *Euro. J. Mech. B/Fluids* **31**, 129–139.

Afsar, M. Z., Sescu, A., & Leib, S. J. 2016 Predictive capability of low frequency jet noise using an asymptotic theory for the adjoint vector Green's function in non-parallel flow. *AIAA Paper #2016-2804.*

Brès, G. A., Nichols, J. W., Lele, S. K. and & Ham, F. 2012 Towards best practices for jet noise predictions with unstructured large eddy simulations. *AIAA Paper* 2012-2965.

Brès, G.A., Ham, F.E., Nichols, J.W. & S.K. Lele, Unstructured large eddy simulations of supersonic jets. *AIAA J.* (In Press).

Garabedian, P. R. 2008 *Partial Differential Equations*. AMS Chelsea Publishing.

Goldstein, M. E. 1975 The low frequency sound from multipole sources in axisymmetric shear flows with application to jet noise. *J. Fluid Mech.* **70**, 595–604.

Goldstein, M. E. 2003 A generalized acoustic analogy. *J. Fluid Mech.* **488**, 315–333.

Goldstein, M. E. & Leib, S. J. 2008 The aero-acoustics of slowly diverging supersonic jets. *J. Fluid Mech.* **600**, 291–337.

Goldstein, M. E., Sescu, A., & Leib, S. J. 2012 Effect of non-parallel mean flow on the Green's function for predicting the low frequency sound from turbulent air jets. *J. Fluid Mech.* **695**, 199–234.

Karabasov, S. A., Afsar, M. Z., Hynes, T. P., Dowling, A.P., McMullan, W. A., Pokora, C. D., Page, G. J. & McGuirk, J. J. 2010 Jet noise: acoustic analogy informed by large eddy simulation. *AIAA J.* **48**, 1312–1325.

Karabasov, S. A., Bogey, C & Hynes. 2011 Computation of noise of initially laminar jets using a statistical approach for the acoustic analogy: application and discussion. *AIAA Paper* 2011-2929.

Leesshafft, L., Huerre, P., Sagaut, P. & Terracol, M. 2006 Nonlinear global modes in hot jets. *J. Fluid Mech.* **554**, 393–409.

Morse, P. M. & Feshbach, H. 1953 *Methods of Theoretical Physics*. McGraw-Hill.

Schlinker, R. H., Simonich, J. C., Reba, R. A., Colonius, T., Gudmundsson, K. & Ladeinde, F. 2012 Supersonic jet noise from round and chevron nozzles: experimental studies. *AIAA Paper* 2009-3257.

Van Dyke, M. 1975 *Perturbation Methods in Fluid Mechanics* . The Parabolic Press.

Wu, X. & Huerre, P. 2009 Low-frequency sound radiated by a nonlinearly modulated wavepacket of helical modes on a subsonic circular jet. *J. Fluid Mech.* **637**, 173–211.